PLOS PATHOGENS

RESEARCH ARTICLE

Unmasking cellular response of a bloom-forming alga to viral infection by resolving expression profiles at a single-cell level

Shilo Rosenwasser[1,2]*, Uri Sheyn[1], Miguel J. Frada[1,3,4], David Pilzer[5], Ron Rotkopf[6], Assaf Vardi[1]*

1 Department of Plant and Environmental Sciences, Weizmann Institute of Science, Rehovot, Israel, **2** The Robert H. Smith Institute of Plant Sciences and Genetics in Agriculture, The Hebrew University, Rehovot, Israel, **3** The Interuniversity Institute for Marine Sciences, Eilat, Israel, **4** Department of Ecology, Evolution and Behavior, Silberman Institute of Life Sciences, The Hebrew University of Jerusalem, Jerusalem, Israel, **5** Genomic Technologies Unit, Weizmann Institute of Science, Rehovot, Israel, **6** Bioinformatics and Biological Computing Unit, Weizmann Institute of Science, Rehovot, Israel

* shilo.rosenwaser@mail.huji.ac.il (SR); assaf.vardi@weizmann.ac.il (AV)

Check for updates

OPEN ACCESS

Citation: Rosenwasser S, Sheyn U, Frada MJ, Pilzer D, Rotkopf R, Vardi A (2019) Unmasking cellular response of a bloom-forming alga to viral infection by resolving expression profiles at a single-cell level. PLoS Pathog 15(4): e1007708. https://doi.org/10.1371/journal.ppat.1007708

Editor: Nigel Harry Grimsley, CNRS, FRANCE

Received: January 17, 2019

Accepted: March 15, 2019

Published: April 24, 2019

Copyright: © 2019 Rosenwasser et al. This is an open access article distributed under the terms of the Creative Commons Attribution License, which permits unrestricted use, distribution, and reproduction in any medium, provided the original author and source are credited.

Data Availability Statement: All relevant data are within the paper and its Supporting Information files.

Funding: This research was supported by the European Research Council (ERC) StG (INFOTROPHIC grant no. 280991) and CoG (VIROCELLSPHERE grant no. 681715) awarded to AV. The funders had no role in study design, data collection and analysis, decision to publish, or preparation of the manuscript.

Competing interests: The authors have declared that no competing interests exist.

Abstract

Infection by large dsDNA viruses can lead to a profound alteration of host transcriptome and metabolome in order to provide essential building blocks to support the high metabolic demand for viral assembly and egress. Host response to viral infection can typically lead to diverse phenotypic outcome that include shift in host life cycle and activation of anti-viral defense response. Nevertheless, there is a major bottleneck to discern between viral hijacking strategies and host defense responses when averaging bulk population response. Here we study the interaction between *Emiliania huxleyi*, a bloom-forming alga, and its specific virus (EhV), an ecologically important host-virus model system in the ocean. We quantified host and virus gene expression on a single-cell resolution during the course of infection, using automatic microfluidic setup that captures individual algal cells and multiplex quantitate PCR. We revealed high heterogeneity in viral gene expression among individual cells. Simultaneous measurements of expression profiles of host and virus genes at a single-cell level allowed mapping of infected cells into newly defined infection states and allowed detection specific host response in a subpopulation of infected cell which otherwise masked by the majority of the infected population. Intriguingly, resistant cells emerged during viral infection, showed unique expression profiles of metabolic genes which can provide the basis for discerning between viral resistant and susceptible cells within heterogeneous populations in the marine environment. We propose that resolving host-virus arms race at a single-cell level will provide important mechanistic insights into viral life cycles and will uncover host defense strategies.

Author summary

Almost all of our current understanding of the molecular mechanisms that govern host-pathogen interactions in the ocean is derived from experiments carried out at the

population level, neglecting any heterogeneity. Here we used a single cell approach to unmask the phenotypic heterogeneity produced within infected populations of the cosmopolitan bloom-forming alga *Emiliania huxleyi* by its specific lytic virus. We found high variability in expression of viral genes among individual cells. This heterogeneity was used to map cells into their infection state and allowed to uncover a yet unrecognized host response. We also provide evidence that variability in host metabolic states provided a sensitive tool to decipher between susceptible and resistant cells.

Introduction

Marine viruses are recognized as major ecological and evolutionary drivers and have immense impact on the community structure and the flow of nutrients through marine microbial food webs [1–5]. The cosmopolitan coccolithophore *Emiliania huxleyi* (Prymnesiophyceae, Haptophyta) is a widespread unicellular eukaryotic alga, responsible for large oceanic blooms [6, 7]. Its intricate calcite exoskeleton accounts for ~1/3 of the total marine $CaCO_3$ production [8]. *E. huxleyi* is also a key producer of dimethyl sulfide [9], a bioactive gas with a significant climate-regulating role that seemingly enhances cloud formation [10]. Therefore, the fate of these blooms may have a critical impact on carbon and sulfur biogeochemical cycles. *E. huxleyi* spring blooms are frequently terminated as a consequence of infection by a specific large dsDNA virus (*E. huxleyi* virus, EhV) [11, 12]. The availability of genomic and transcriptomic data and a suite of host isolates with a range of susceptibilities to various EhV strains, makes the *E. huxleyi*-EhV a trackable host-pathogen model system with important ecological significance [13–20].

Recent studies demonstrated that viruses significantly alter the cellular metabolism of their host either by rewiring of host-encoded metabolic networks, or by introducing virus-encoded auxiliary metabolic genes (vAMG) which convert the infected host cell into an alternate cellular entity (the virocell [21]) with novel metabolic capabilities [22–27]. A combined transcriptomic and metabolomic approach taken during *E. huxleyi*-EhV interaction revealed major and rapid transcriptome remodeling targeted towards *de novo* fatty acid synthesis [18] fueled by glycolytic fluxes, to support viral assembly and the high demand for viral internal lipid membranes [28, 29]. Lipidomic analysis of infected *E. huxleyi* host and purified EhV virions further revealed a large fraction of highly saturated triacylglycerols (TAGs) that accumulated uniquely within distinct lipid droplets as a result of virus-induced lipid remodeling [27]. The EhV genome encodes for a unique vAMG pathway for sphingolipid biosynthesis, never detected before in any other viral genome. Biochemical characterization of EhV-encoded serine palmitoyl-CoA transferase (SPT), a key enzyme in the sphingolipid biosynthetic pathway, revealed its unique substrate specificity which resulted in the production of virus-specific glycosphingolipids (vGSLs) composed of unusual hydroxylated C17 sphingoid-bases [30]. These viral-specific sphingolipids are essential for viral assembly and infectivity and can induce host programmed cell death (PCD) during the lytic phase of infection [14, 31]. Indeed, EhV can trigger hallmarks of PCD, including production of reactive oxygen species (ROS), induction of caspase activity, metacaspase expression, changes in ultrastructure features and compromised membrane integrity [32–34].

The high metabolic demand for building blocks required to support synthesis, replication and assembly of large viruses with high burst size as EhV [34–36] point to high dependence of viruses on their host metabolic state for optimal replication [21, 37]. Consequently, heterogeneity in host metabolic states as a result of complex interactions between nutrient availability

and stress conditions may affect the infection dynamics. However, almost all of our current understanding of the molecular mechanisms that govern host-virus interactions in the ocean, is derived from experiments carried out at the population level, assuming synchrony and uniformity of the cell populations and neglecting any heterogeneity. Additionally, averaging the phenotypes of a whole population hinders the investigation of essential life cycle strategies to evade viral infection that can be induced only by rare subpopulations [38]. Understanding microbial interactions at a single-cell resolution is an emerging theme in microbiology. It enables the detection of complex heterogeneity within microbial populations and has been instrumental to identify novel strategies for acclimation to stress [39–41]. The recent advancement of sensitive technologies to detect gene expression from low input-RNA allows quantification of heterogeneity among cells by analyzing gene expression at the single cell level [42, 43]. High-throughput profiling of single-cell gene expression patterns in mammalians and plant cells led to the discovery of new cell types, detection of rare cell subtypes, and provides better definition and cataloging of developmental phases in high resolution [44–48]. Importantly, the role of cell-to-cell communication and variability in controlling infection outcomes has only been recently demonstrated in cells of the mammalian immune system in response to bacterial pathogens [49–52]. Cell-to-cell variability in host response to viral infection was observed in several mammalian viruses and was attributed to several factors, including intrinsic noise (e.g. stochasticity of biochemical interactions involved in the infection process), the number of viral genomes initiating the infection process and the specific cell-state before the infection [52–58]. The existence of cell-to-cell variability during infection suggests that key events in host response are masked by conventional bulk cell expression profiling and that detection of gene expression on single cell resolution may uncover hidden host responses. Recently, simultaneous detection of host and pathogen gene expression profile was suggested as a powerful tool used to gain a better understanding of the molecular mechanisms underlying the infection process and to identify host defense responses [21, 59–61].

Here, we used multiplex single cell qPCR to quantify the dynamics of host and virus gene expression profiles of individual cells during infection of *E. huxleyi* populations. We provide strong evidence for heterogeneity within the population and discern between cells at different infection states based on their viral gene expression signatures. We unravel an unrecognized phase of early host response that preceded viral gene expression within infected cells. We suggest that examining host and virus gene expression profiles at the single cell resolution allows to infer the temporal dynamic of the infection process, thereby it serves as an attractive approach to decipher the molecular mechanism underlying host-virus interaction.

Results and discussion

To examine the variability within infected *E. huxleyi* cells, we measured the expression levels of selected host and viral genes over the course of infection at a single-cell resolution. Cells were isolated during infection of *E. huxleyi* CCMP2090 at different phases, at 0, 2, 4, 24 hours post infection (hpi) (Fig 1, Fig A in S1 Text). We used the C1 single-cell Auto Prep System to sort and extract RNA from single *E. huxleyi* cells during viral infection by EhV201. The presence of a single cell captured in an individual isolation chamber was confirmed by microscopic inspection of emitted chlorophyll auto-fluorescence (Fig 2A). In order to detect variability in viral infection states, we conducted simultaneous measurements of expression profiles of host and virus genes at a single-cell level by using multiplexed qPCR. We selected viral genes encoding for sphingolipid biosynthesis as well as gene markers for early and late infection [18, 62]. Selected genes involved in host metabolic pathways were targeted based on previous reports which demonstrated their functional role during infection, including primary metabolism

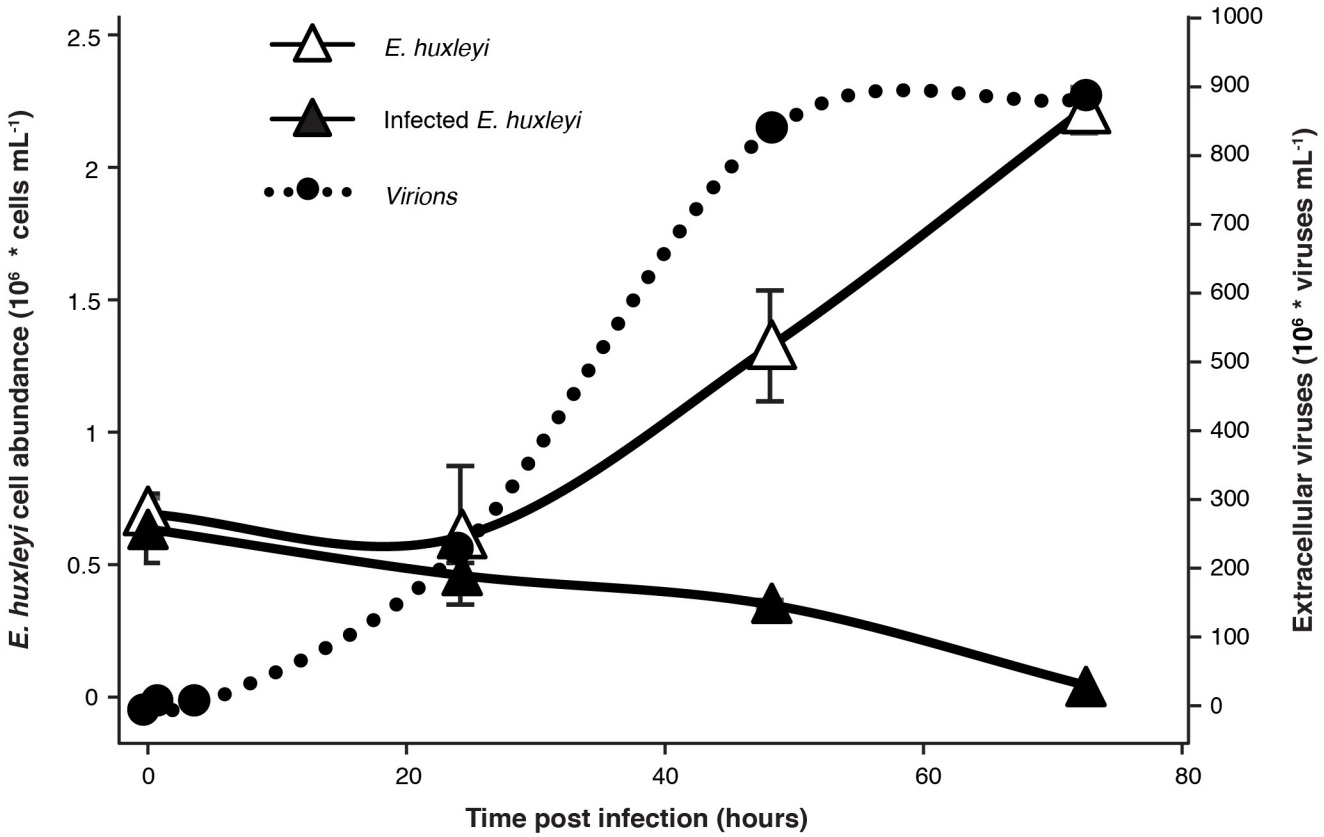

Fig 1. Infection dynamics of *E. huxleyi* by its specific virus EhV. *E. huxleyi* CCMP2090 culture was infected by the EhV201 lytic virus and compared with uninfected control cells. Host cell abundance and production of extracellular viruses were monitored using flow-cytometry. (mean ± SD, n = 3, at least 6000 cells were measured at each time point).

https://doi.org/10.1371/journal.ppat.1007708.g001

(glycolysis, fatty acid biosynthesis), sphingolipid and terpenoid metabolism, autophagy and antioxidant genes [18, 27, 33, 34]. In addition, we examined the expression of host genes associated with life cycle [63], meiosis and PCD [32] that exhibited induction during infection. (In total expression of 107 host genes and 10 viral genes was measured, see S1 Table for primers list).

To test for the sensitivity in detection of gene expression on a single cell level, we spiked-in, to each C1 well, a set of External RNA Controls Consortium (ERCC) molecules that span a wide range of RNA concentrations (from ~0.5 to ~100 molecules per well). We subsequently quantified their concentration using similar qPCR amplification setup as used for the host and virus genes. Pairwise correlation between spike concentrations and Et (Et = 30-Ct) values obtained from the qPCR was >0.98 (Pearson correlation coefficient, p-value = $4.2 10^{-12}$, Fig 2B). We found a highly sensitive level of detection with 40% probability to detect an RNA spike that is at a level of 1 molecule per sample (Fig 2C), similar to the detection level reported for mammalian cells [64]. Mean expression of viral and host genes in all examined cells were found to be 11.8 ± 4.0 and 6.96 ± 2.5 (Et values ± SD), respectively (Fig 2D).

We detected a high variability in viral expression profiles among individual cells within the same infected population. For example, heterogeneity in the expression levels of virus-encoded ceramide synthase (*vCerS*, EPVG_00014), a key enzyme in sphingolipid biosynthesis [18, 30] was detected during early phase of infection (2 and 4 hpi of CCMP2090, Fig 3A). Similar results were obtained for the average expression of 10 viral genes (Fig 3B). At the onset of viral

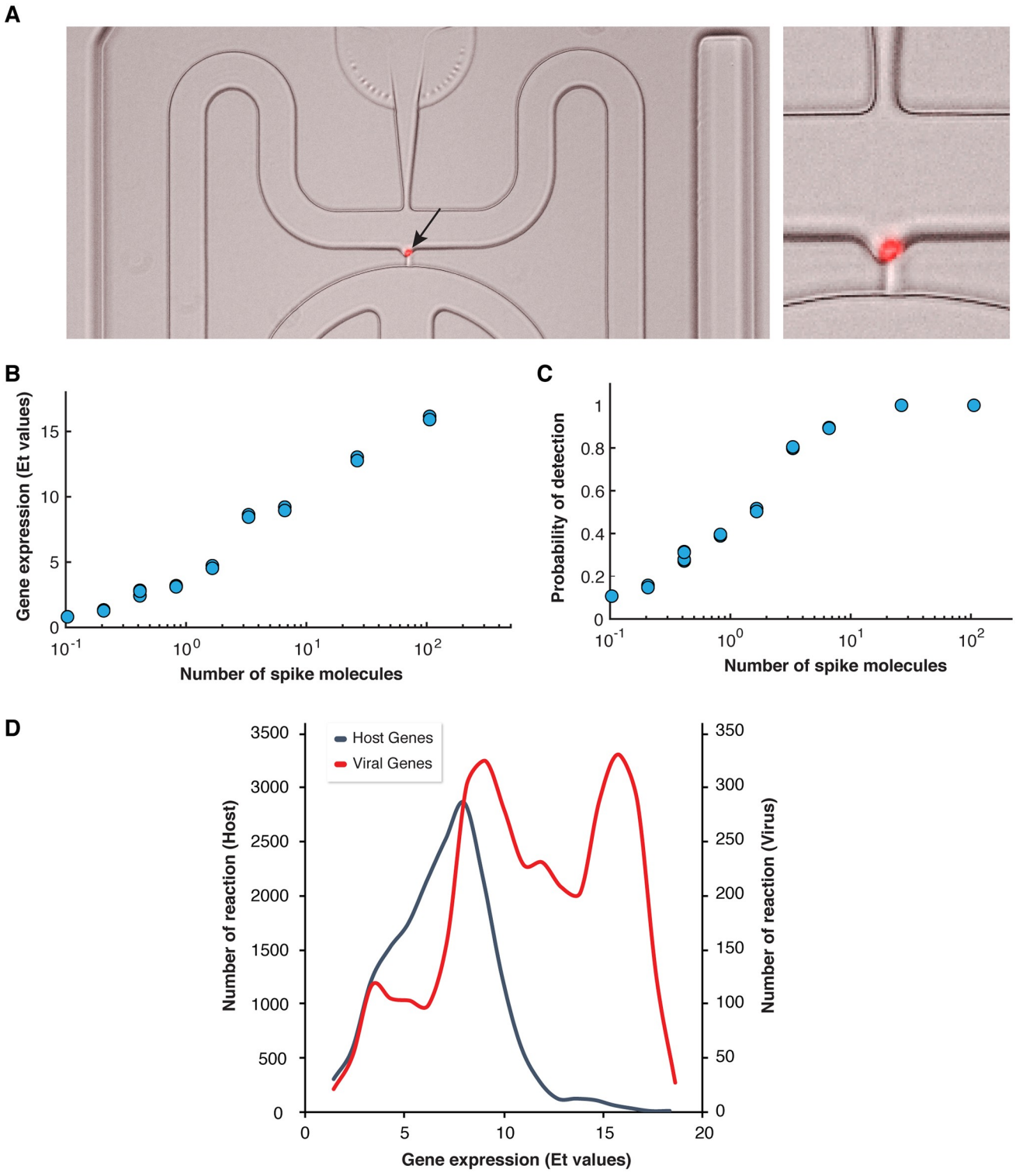

Fig 2. Host and virus gene expression profiling at a single cell level. (A) Automated microfluidic capture of a single *E. huxleyi* cell in the C1 chip (red: chlorophyll autoflouresence, indicated by a black arrow), the image on the right is a zoom into the image of a single cell. (B,C) Examination of detection level of single-cell gene expression analysis. A set of ERCC RNA molecules were spiked to each C1 well and their level was determined using multiplex qPCR. (B) The fraction of wells with positive qPCR reaction (Ct < 30) for each examined spike. (C) The correlation between the average level of expression (Et = 30-Ct) value and the number of spike molecule. (D) Distribution of host and virus genes expression among individual cells. The average expression values of host and viral genes among isolated single cells was calculated and the distribution is presented.

https://doi.org/10.1371/journal.ppat.1007708.g002

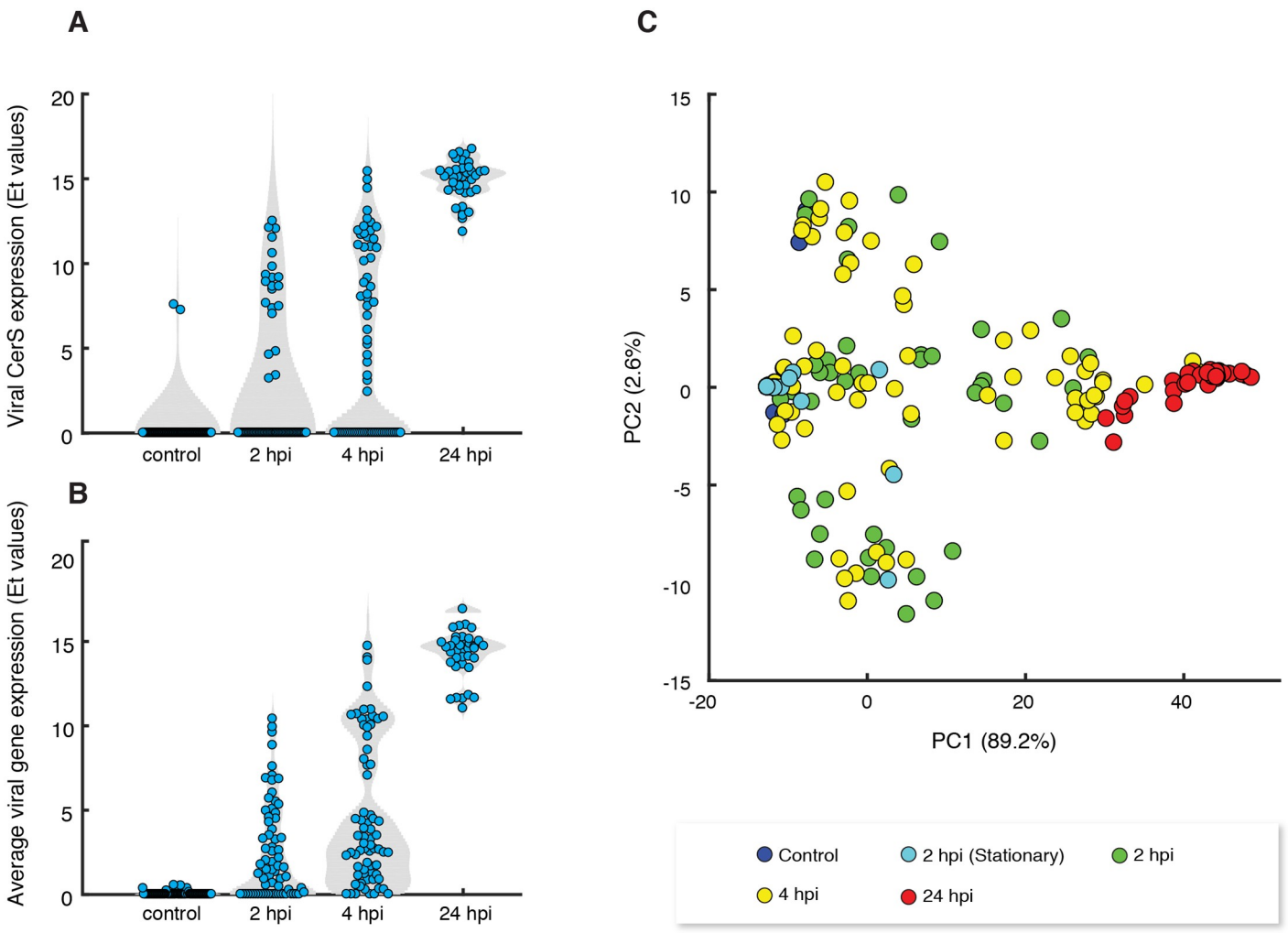

Fig 3. Single-cell analysis of infected population unmasks heterogeneity in viral gene expression profiles. (A) Violin plots of the expression value (Et) of viral ceramide synthase (vCerS, EPVG_14, Gene bank: AET97902.1) at different hours post infection (hpi) of CCMP2090 cells infected by EhV201. (B) Violin plots of the mean expression value of 10 viral genes at different times post infection of CCMP2090 cells with EhV201. (C) Principal component analysis (PCA) plots of gene expression profiles of 10 viral genes derived from 323 individual *E. huxleyi* cells that were isolated from infected CCMP2090 cultures at different hpi.

https://doi.org/10.1371/journal.ppat.1007708.g003

lytic phase (24 hpi), all of the examined cells showed high viral gene expression (Fig 3A and 3B), suggesting that viruses eventually infected all of the examined host cells. Nevertheless, we cannot exclude the existence of a rare subpopulation that did not express viral genes. The observed heterogeneity in viral expression is probably not a result of infection with defective viruses since no viral expression was detected using UV-inactivated virions (Fig B in S1 Text). A possible source of the observed heterogeneity is the asynchronous state of cells in the initial culture resulting in a difference in cell cycle phase and metabolic state between individual cells.

Principal component analysis (PCA) of viral gene expression among individual host cells showed that infected cells are distributed across distinct states of viral expression levels (Fig 3C). All viral genes had positive and similar coefficients for the PC1 component which captures >90% of the variability of viral gene expression and found to be highly correlated to the average viral infection level (r = 0.99, Pearson linear correlation). These results demonstrate that PC1 reflected the intensity of viral infection. Accordingly, we used the score value of PC1

as an index for the level of expression of viral genes in each individual cell and termed it "infection index".

We further realized that averaging host gene expression over the course of infection might hinder our ability to observe the initial response of the host to viral infection and that single-cell analysis could significantly increase the resolution for sensitive detection of host response at this early stage of infection. We therefore re-ordered infected cells based on their viral infection index (PC1), rather than the actual time of infection (i.e. hpi), resulting in "pseudotemporal" hierarchy of single cells (Fig 4). Intriguingly, we unmasked a fraction of cells that were exposed to the virus but did not exhibit any detectable expression of viral genes. These cells had similar infection index values as control cells, with PC1 values < -10 (Fig 4A). We found that 33/179 (17%) of infected cells of CCMP2090 were at this distinct "lag phase" of viral infection. These individual cells were analyzed for their respective host gene expression levels based on a sliding window approach (Fig 4B and 4C), as it is less sensitive to technical noise, often observed in single cell data. We also used a statistical model to test for genes that are differentially expressed at these early stages of viral infection. This model incorporates the two types of heterogeneity that usually appear in single cell data, namely, the percentage of cells expressing a gene in a given population (e.g. Et value > 0) and the variability in expression levels in cells exhibiting positive expression values [65]. Up-regulation of several host genes in infected cells was detected in this subpopulation (Fig 4C and S2 Table). An intriguing example is the *metacaspase-2* gene ($p = 0.0000027$) which was previously suggested to be induced and recruited during EhV lytic phase and activation of *E. huxleyi* PCD [32]. We also found early induction of triosephosphate isomerase (*TPI*, $p = 0.00063$) and phospholipid:diacylglycerol acyltransferase (*PDAT*, $p = 0.0018$) which are involved in glycolysis and TAG biosynthesis respectively. In addition, genes involve in autophagy [34] and *de novo* sphingolipid biosynthesis [18, 30] were detected in this unique early phase of host response. Since major alteration in these specific metabolic pathways were recently shown to be essential for EhV infection [14, 18, 20, 21, 27, 30, 31, 33, 34], early induction of these pathways may serve as an effective viral strategy to prime optimal infection. Alternatively, this phase of early host response prior to viral gene expression may represent a newly unrecognized phase of immediate host anti-viral defense response. At the late stages of infection (infection index >10), we observed induction of several meiosis-related genes, including *HOP1* and *MND*, two *SPO11* homologues and *MYB* in CCMP2090 (Fig 4B). These results are in agreement with previous studies that suggested a phenotype switch of *E. huxleyi* to evade viral infection [38] and propose the induction of meiosis-related genes as part of transcriptomic reprogramming of during infection [63].

Further inspection of the PCA analysis showed the cells exhibiting low to moderate level of PC1 were highly variable in their PC2 level (Fig 3C). To identify the viral genes that contribute to this variability, we further examined the correlation coefficients between the viral gene expression and principal components 2 (PC2). Interestingly, this analysis revealed a positive correlation ($r = 0.53$) between PC2 and the expression level of viral RNA polymerase gene (EPVG_00062) which was previously reported to be expressed at early-mid phases of infection [18, 62], while a negative correlation ($r = -0.44$) was found for a viral gene (EPVG_00010) that is known to be expressed at late phases of infection. Accordingly, cells with low PC2 levels expressed EPVG_00010 and not EPVG_00062, while cells with high PC2 values exhibited the opposite trend (as compared with Fig 5A and 5B).

To further characterize host gene expression during different phases of infection, we manually clustered CCMP2090 cells according to their infection index (PC1) and the expression of either early or late viral genes (PC2) (Fig 5C) and examined the expression of host metabolic genes in these clusters (Fig 5D). This analysis showed that induction of most of host metabolic genes occurred in cells that expressed predominantly late viral genes (Fig 5D, CL5,

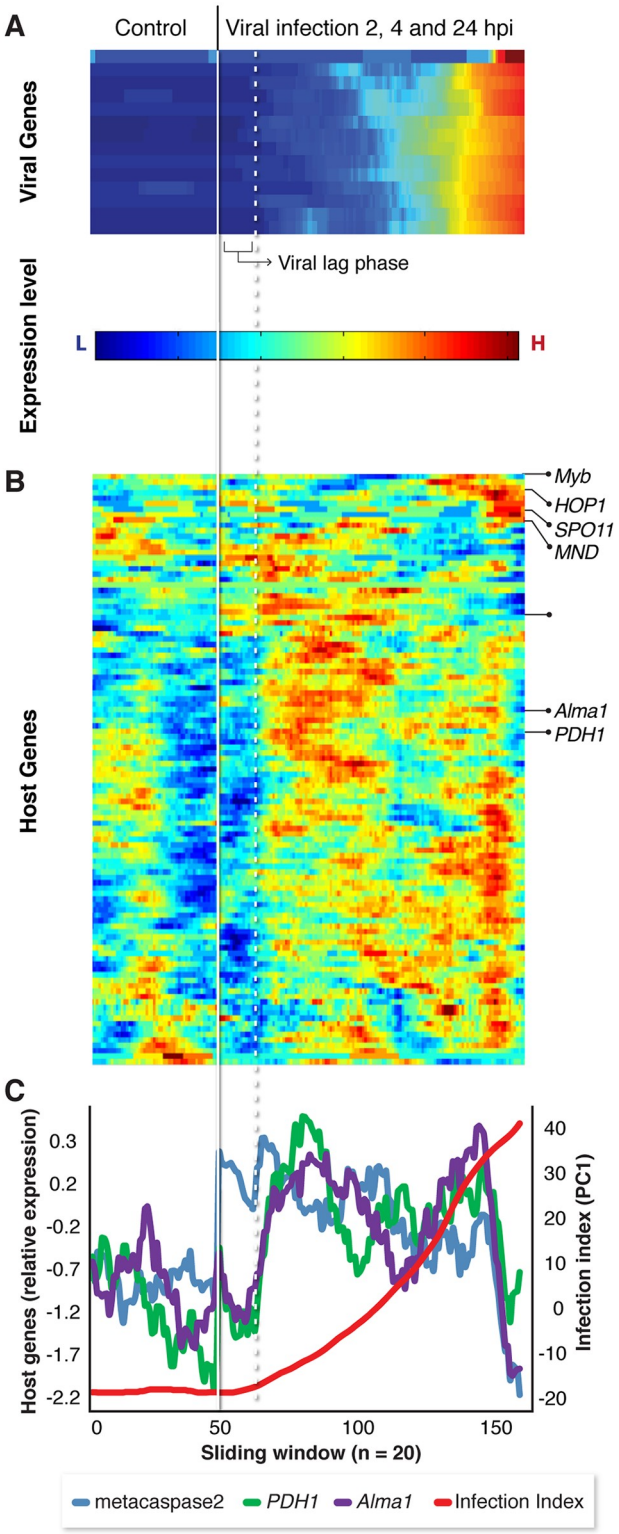

Fig 4. Host-virus co-expression patterns across viral infection states. Cells were re-ordered based on their infection index (PC1 from Fig 3C) to reconstruct pseudotemporal separation of the infection process. (A, B) Clustogram representation of the average expression value of viral (A) and host (B) genes across the infection dynamics of CCMP2090 using a sliding window approach (window size = 20 cells). (C) Expression profile of selected host genes along the viral infection index (PC1) in the sliding windows of 20 cells reveals early induction of host genes prior to

viral gene expression. Solid line represents the border between uninfected cells and infected cells which were analyzed separately. The dotted line represents the separation between cell expressing viral genes and cells that do not express viral genes in the population of infected culture.

https://doi.org/10.1371/journal.ppat.1007708.g004

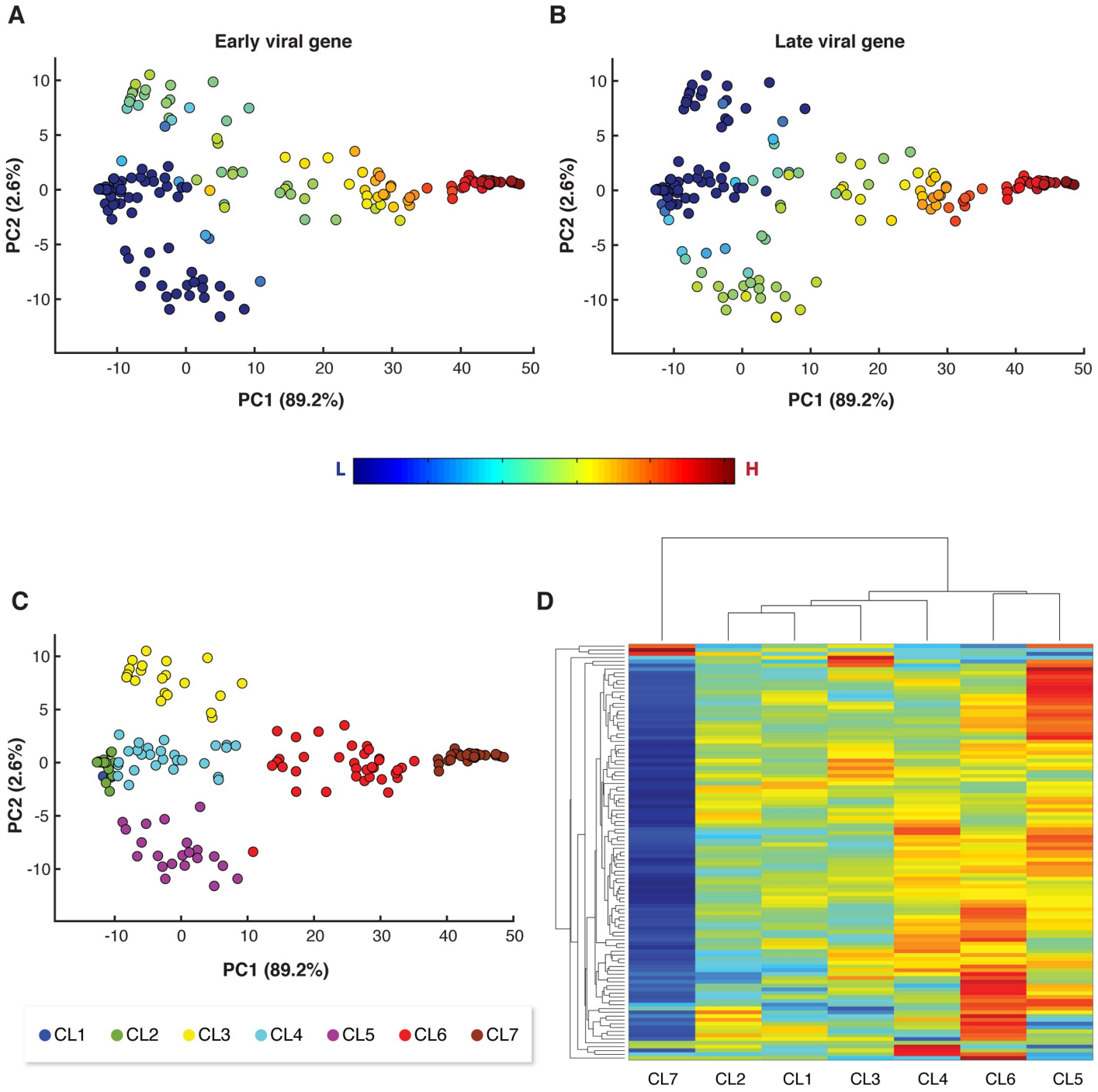

Fig 5. Viral expression is associated with induction of host metabolic genes at distinct phases of infection. (A, B) The same PCA plots as in Fig 3C were colored based on the expression level of specific viral genes (Et values) that are associated with early-mid (A) and late (B) phases of viral infection (EPVG_00062 and EPVG_00010, respectively). (C) The same PCA plots as in Fig 3C were colored based on newly defined clusters. Cells were clustered manually based on their infection index (PC1) and PC2 scores. (D) Clustorgam representation of expression values of 107 host metabolic genes across the different clusters as defined in (C).

https://doi.org/10.1371/journal.ppat.1007708.g005

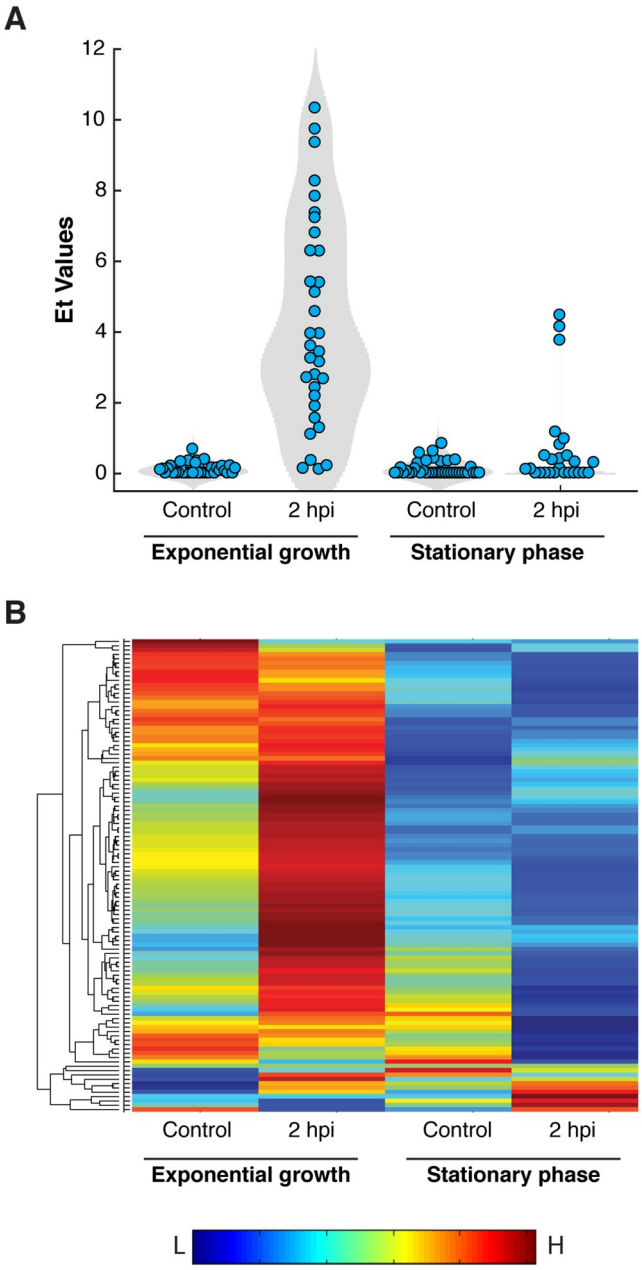

Fig 6. Low viral gene expression in *E. huxleyi* cells at stationary phase is associated with down-regulation of host metabolic genes. (A) Violin plots of the mean expression of viral genes in individual exponential and stationary cells at 2 hpi and in uninfected cells (Control). (B) Clustorgam representation of the average expression values of 109 host metabolic genes in individual exponential and stationary cells at 2 hpi and in uninfected cells.

https://doi.org/10.1371/journal.ppat.1007708.g006

-10<PC1<10, PC2>-5) and in cells with moderate expression of viral genes (Fig 5D, CL6, 10<PC1<36). Down-regulation of many host genes was found in cells exhibiting high viral expression (Fig 5D, CL7, PC1>37), suggesting that these cells were at the final stages of infection.

In order to further explore the link between optimal host metabolic state and efficient viral infection, we infected CCMP2090 stationary culture and subjected single cells to dual gene expression analysis at 2 hpi (Fig 6A). While most of the exponential growing cells exhibited

viral expression, we detected only moderate viral expression in 3/27 (11%) of the stationary phase cells (Fig 6A), while the rest of the cells had viral expression patterns similar to uninfected cells (control). In parallel, stationary phase cells (either control or infected) exhibited down-regulation of most of the examined host metabolic genes, in contrast to their general up-regulation in infected exponential phase cells (Fig 6B). These data suggest that the cell-to-cell variability in host metabolic state may play important role in determining susceptibility to infection by large viruses with high metabolic demand. "Kill the Winner" is a key theory in microbial ecology which suggests that viruses shape diversity of microbial populations by infecting the most dominant proliferative host [66]. We propose that "Kill the Winner" may even act within isogenic populations based on the variability in the metabolic state, which will lead to differential susceptibility to viral infection, forming continuous host-virus co-existence [67]. It is possible that cell-to-cell heterogeneity in the metabolic activity is shaped by the trade-off between complex abiotic stress conditions (e.g. nutrient availability [68–70] and light regime [71]) and biotic interactions (e.g. bacterial pathogenicity [72]), and may result in differential susceptibility to viral infection in the marine environment.

We further investigated whether uninfected susceptible and resistant *E. huxleyi* cells exhibited altered expression profiles in the host metabolic genes that showed variable expression during infection (S3 Table). We exposed *E. huxleyi* cultures to viral infection and isolated cells that acquired resistance to subsequent viral infection of diverse EhV isolates (Fig 7A, [63]). We compared the expression profiles of recovered resistant cells (n = 18) to their mother cells that were highly susceptible to viral infection (n = 76). The tendency of resistant cells to aggregate make it difficult to isolate single cells, therefore for these analysis also included doublet cells. Intriguingly, resistant and susceptible cells tend to cluster distinctively along the PC2 dimension (Fig 7B). Among the genes that drive the separation along the PC2 dimension and were differentially expressed in resistant and susceptible cells were *TPI*, diphosphomevalonate decarboxylase (*MVD1*) and *ceramidase-3* (Fig 7C) which are key enzymes in glycolysis, terpenoid and sphingolipid metabolism, respectively. Since *de novo* ceramide biosynthesis is uniquely encoded in the EhV genome, activation of ceramidase may serve as an anti-viral host response [18, 30]. Interestingly resistant cells also exhibited high expression of *metacaspase2* which was also highly expressed in cells with no viral expression in early phase of infection (Fig 7C). This data suggests that susceptibility to viral infection has a clear signature in expression profiles of host genes detected on a single-cell level.

Although the mechanism for resistance of *E. huxleyi* to viral infection requires further investigations, the differential regulation of host metabolic genes suggests a unique specialized metabolism that differs from that of susceptible cells [73–75]. Future single-cell RNA-seq transcriptomic studies will provide high throughput identification of gene markers that are specific for resistant strains as well as new mechanistic insights into the molecular basis for resistance mechanisms.

Tracking host-virus dynamics at the single cell resolution provides a novel approach to characterize the continuum viral infection states and host responses which is commonly masked in whole population analysis [76]. By applying dual gene expression profiling during algal host-virus interactions, we uncovered an early host transcriptional responses. This newly defined phase can result in different scenarios including, resistant cells, cells infected by defective virions, cells exposed to chemical cues released during infection and cells at the very early stage of infection. The new ability to define distinct "infection states" on a pseudo-temporal manner can provide valuable information regarding the dynamics of active viral infection in "real time" in the natural environment. Clustering of individual cells based on their specific transcriptomic signatures will uncover the relationship between host metabolic states and specific phenotypes associated with differential levels of viral infection or modes of resistance in

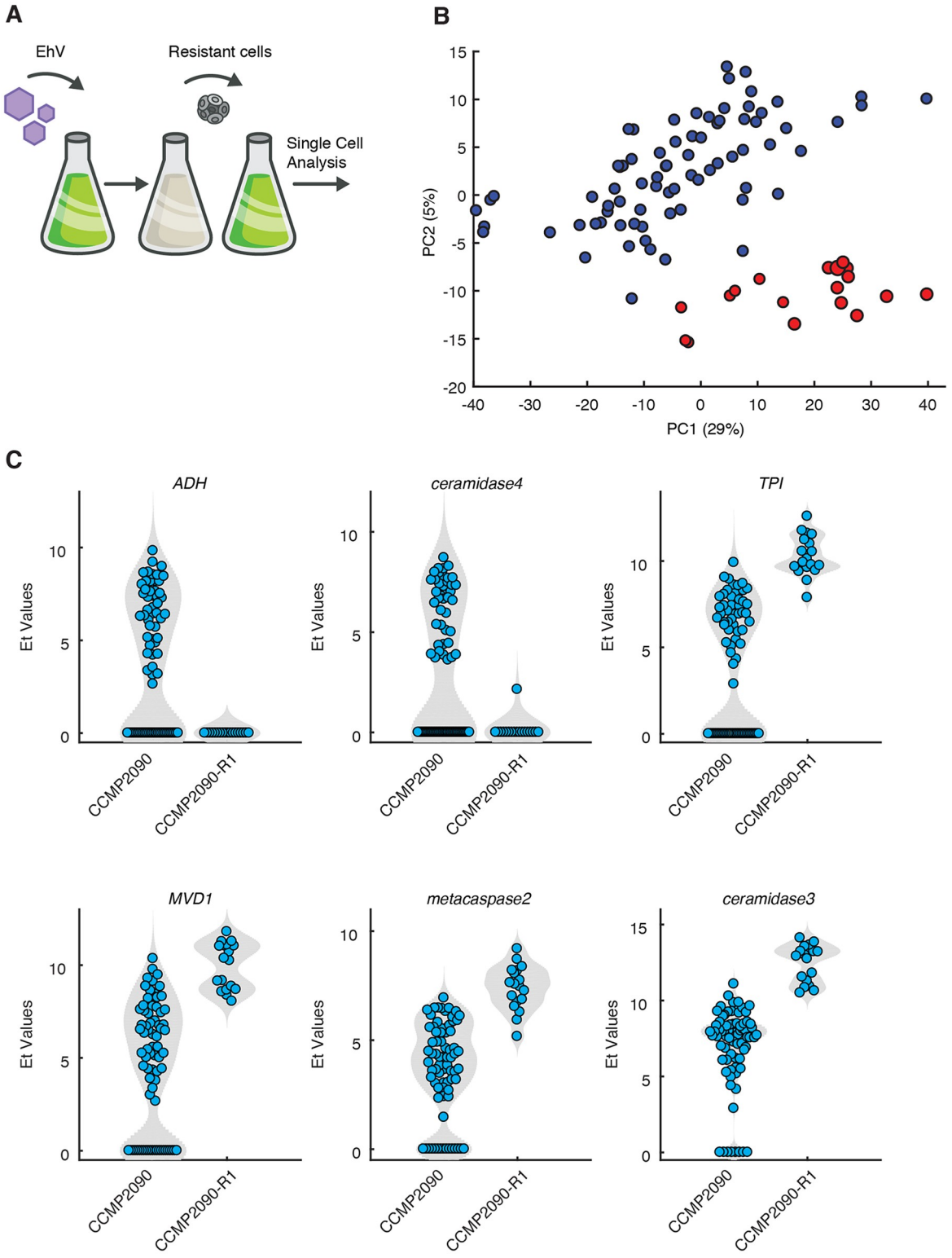

Fig 7. Differential expression of host genes on a single-cell level in virus-susceptible and virus-resistant cells. (A) Virus-resistant cells were isolated from infected CCMP2090 cells. (B) PCA plot of gene expression profiles of 93 host metabolic genes in 94 individual *E. huxleyi* cells that were isolated from the sensitive CCMP2090 and resistant CCMP2090 culture (CCMP2090-R). Doublet cells are visualized by slightly bigger dots.(C) Violin plots of selected host genes that highly contributed to the separation of cells along PC2. The SingleCellAssay R package [62] was used to test significant changes in gene expression and all presented genes had *p-value* < 0.05 of hurdle test (See S3 Table).

https://doi.org/10.1371/journal.ppat.1007708.g007

natural populations. *In situ* quantification of the fraction of infected cells, their infection and metabolic states and the fraction of resistant cells will provide important insights into the infection dynamics and may provide fundamental understating of host-virus co-existence strategies in the ocean. Resolving host-virus interaction on a single cell will promote discovering of novel sensitive biomarkers to assess the ecological impact of marine viruses and their role in regulating the fate of algal blooms in the ocean.

Methods

Culture growth and viral infection dynamics

Cells of the non- calcified CCMP2090 *E. huxleyi* strain were cultured in K/2 medium [77] and incubated at 18˚C with a 16:8 h light– dark illumination cycle. A light intensity of 100 μM photons·m^{-2}·s^{-1} was provided by cool white LED lights. Experiments were performed with exponential phase ($5{\cdot}10^5$–$1{\cdot}10^6$ cells·ml-1) or stationary phase ($5{\cdot}10^6$ cells·ml-1) cultures. *E. huxleyi* virus EhV201 (lytic) used for this study was isolated originally in [12]. *E. huxleyi* was infected with a 1:50 volumetric ratio of viral lysate to culture. By using plaque assay we counted the infectious particles of EhV lysate commonly use in our lab and found that the concentration of infectious particles is around $2.5^{*}10^7$–$5^{*}10^7$ ·ml^{-1} (which is around 20% of particles counted by flow-cytometry). Thus, at the time of infection, there is about one infectious particle per cell.

For virus deactivation, 15 ml of 0.45 μm filtered viral lysate was placed in a Petri plate and radiated on uvitec (Cambridge, UK) ultra-violate light table, with 312 nm light for 15 min. To evaluate the infectivity of the deactivated viral lysate plaque assay was performed indicating a reduction of 8 fold in the number of infective particle per mL in the deactivated (~20 infective particles per mL) in comparison to the active viral lysate (10^8 infective particles per mL). For single-cell analysis, *E. huxleyi* cells were concentrated to $2.5{\cdot}10^6$ cells·ml-1 by gentle centrifugation (3000 RPM, 3 min) prior to single-cell isolation. To compare between viral infection in exponential and stationary phases, stationary phase cells were diluted to similar concentration of exponential phases cells using stationary conditioned medium ($5{\cdot}10^5$–$1{\cdot}10^6$ cells·ml-1) and then infected by EhV. The growth dynamics of *E. huxleyi* CCMP2090 were monitored in seawater-based K/2 medium in control conditions and in the presence of the lytic viral strain EhV201. Resistant single cells were isolated after infection by mouth-pippetting over multiple passages through fresh medium under an inverted microscope as described in [63]. Single isolates were maintained in K/2 medium.

Enumeration of cell and virus abundance

Cells were monitored and quantified using a Multisizer 4 Coulter counter (Beckman Coulter, Nyon, Switzerland). For extracellular viral production, samples were filtered using 0.45 μM PVDF filters (Millex-HV, Millipore). Filtrate was fixed with a final concentration of 0.5% glutaraldehyde for 30 min at 4˚C, then plunged into liquid nitrogen, and stored at -80˚C until analysis. After thawing, 2:75 ratio of fixed sample was stained with SYBER gold (Invitrogen) prepared in Tris–EDTA buffer as instructed by the manufacturer (5 μl SYBER gold in 50 mL Tris–EDTA), then incubated for 20 min at 80˚C and cooled down to room temperature. Flow cytometric analysis was performed with excitation at 488 nm and emission at 525 nm.

Calculation of infectious particles during infection (Fig C in S1 Text) was done by using the most probable number (MPN) method as described in [20]. Briefly, medium was of infected culture was subjected to a series of fivefold dilutions for each sample. Each dilution (10 μl) was then added, in six technical replicates, to 100 μl of exponentially growing *E. huxleyi* cultures in multiwell plates over four or five days. MPN was calculated using the MPNcalc software.

Single-cell Quantitative RT-PCR

Single cells were captured on a C1 STA microfluidic array (5–10 μm cells) using the Fluidigm C1 and imaged on IX71S1F-3-5 motorized inverted Olympus microscope (Tokyo, Japan) to examine chlorophyll autofluorescence (ex:500/20 nm, em:650 nm LP). Only wells that exhibited chlorophyll autofluorescence signal emitted from single cells were further analyzed. External RNA Controls Consortium (ERCC) spikes were added to each well in a final dilution of 1:40,000. Cells were lysed and pre-amplified cDNA was generated from each cell using the Single Cells-to-CT Kit (Life Technologies). Pooled qPCR primers and Fluidigm STA reagents were added according to manufacturer's recommendations. Preamplified cDNA was then used for high-throughput qPCR measurement of each amplicon using a BioMark HD system. Briefly, a 2.7 μl aliquot of each amplified cDNA was mixed with 3 μl of 2X SsoFast EvaGreen Supermix with Low ROX (Bio-Rad) and 0.3 μl of 20X DNA Binding Dye Sample Loading Reagent (Fluidigm), and 5 μl of each sample mix was then pipetted into one sample inlet in a

96.96 Dynamic Array IFC chip (Fluidigm). Individual qPCR primer pairs (50 μM, S1 Table) in a 1.08 μl volume were mixed with 3 μl Assay Loading Reagent (Fluidigm) and 1.92 μl Low TE, and 5 μl of each mix was pipetted into one assay inlet in the same Dynamic Array IFC chip. Subsequent sample/assay loading was performed with an IFC Controller HX (Fluidigm) and qPCR was performed on the BioMark HD real- time PCR reader (Fluidigm) following manufacturer's instructions using standard fast cycling conditions and melt-curve analysis, generating an amplification curve for each gene of interest in each sample (cell). Data was analyzed using Real-time PCR Analysis software (Fluidugm) with the following settings: 0.65 curve quality threshold, linear derivative baseline correction, automatic thresholding by assay (gene), and manual melt curve exclusion. Cycle threshold (Ct) values for each reaction were exported. As seen in other applications of this technology [65], the data had a bimodal distribution with some cells ranging from 2.5 Ct to 30 Ct, and another set of cells with Ct >40. Similar bimodal distribution was also observed for the ERCC spikes. Accordingly, we set the minimal threshold level of detection to 30 Ct and calculated expression threshold values (Et) by linear transformation of the data so that minimal Et was zero (30 Ct). For heat map visualization, expression data was normalized by subtracting the mean of each gene and dividing it with its standard deviation across cells. Single-cell PCR data was analyzed and displayed using MATLAB (MathWorks). Additional statistical analyses were performed using The SingleCellAssay R package [65]. Calculation of number of spike molecule per Fluidigm C1 well was performed according to [64].

Supporting information

S1 Table. List of host and viral genes which their expression level was examined.
(XLSX)

S2 Table. Statistical analysis of single cell gene expression data by the SingleCellAssay R package [62]. Genes with significant altered expression in different viral infection states (p-values <0.05 of hurdle test) are presented.
(XLSX)

S3 Table. Statistical analysis of single cell gene expression data by the SingleCellAssay R package [62]. Genes with significant altered expression in susceptible versus resistant strains (p-values <0.05 of hurdle test) are presented.
(XLSX)

S1 Text. Additional supporting data describing viral gene expression level, extracellular viral abundance and infectivity during EhV infection of *E. huxleyi* cells.
(DOCX)

Acknowledgments

We wish thank Dr. Daniella Schatz and Guy Schleyer from the Vardi lab, Dr. Roi Avraham from the Department of Biological Regulation at the Weizmann Institute of Science and Dr. Noam Stern-Ginossar from the Department of Molecular Genetics at the Weizmann Institute of Science for critical comments on the manuscript and fruitful discussion. We would also like to thank Tal Bigdary from the Design, Photography and Printing Branch at the Weizmann Institute of Science for assistance in designing the graphs for this manuscript.

Author Contributions

Conceptualization: Shilo Rosenwasser, Assaf Vardi.

Data curation: Shilo Rosenwasser, Uri Sheyn, David Pilzer, Ron Rotkopf, Assaf Vardi.

Formal analysis: Shilo Rosenwasser, Uri Sheyn, Miguel J. Frada, David Pilzer, Ron Rotkopf, Assaf Vardi.

Funding acquisition: Assaf Vardi.

Investigation: Shilo Rosenwasser, Uri Sheyn, Miguel J. Frada, David Pilzer, Assaf Vardi.

Methodology: Shilo Rosenwasser, Uri Sheyn, Miguel J. Frada, David Pilzer, Ron Rotkopf, Assaf Vardi.

Software: Ron Rotkopf.

Supervision: Assaf Vardi.

Validation: Shilo Rosenwasser, Assaf Vardi.

Visualization: Shilo Rosenwasser, Uri Sheyn.

Writing – original draft: Shilo Rosenwasser, Assaf Vardi.

Writing – review & editing: Shilo Rosenwasser, Assaf Vardi.

References

1. Bergh O, Borsheim KY, Bratbak G, Heldal M. High abundance of viruses found in aquatic environments. Nature. 1989; 340(6233):467–8. https://doi.org/10.1038/340467a0 PMID: 2755508
2. Suttle CA. Marine viruses—major players in the global ecosystem. Nat Rev Micro. 2007; 5(10):801–12.
3. Fuhrman JA. Marine viruses and their biogeochemical and ecological effects. Nature. 1999; 399 (6736):541–8. https://doi.org/10.1038/21119 PMID: 10376593
4. Wilhelm SW, Suttle CA. Viruses and Nutrient Cycles in the Sea: Viruses play critical roles in the structure and function of aquatic food webs. BioScience. 1999; 49(10):781–8. https://doi.org/10.2307/1313569
5. Weitz JS, Stock CA, Wilhelm SW, Bourouiba L, Coleman ML, Buchan A, et al. A multitrophic model to quantify the effects of marine viruses on microbial food webs and ecosystem processes. ISME J. 2015; 9(6):1352–64. https://doi.org/10.1038/ismej.2014.220 PMID: 25635642
6. Holligan PM, Fernandez E, Aiken J, Balch WM, Boyd P, Burkill PH, et al. A biogeochemical study of the coccolithophore Emiliania huxleyi, in the North Atlantic. Global Biogeochem Cy. 1993; 7:879–900.
7. Taylor AR, Brownlee C, Wheeler G. Coccolithophore cell biology: chalking up progress. Annual review of marine science. 2017; 9:283–310. https://doi.org/10.1146/annurev-marine-122414-034032 PMID: 27814031

8. Iglesias-Rodriguez D, Halloran PR, Rickaby REM, Hall IR, Colmenero-Hidalgo E, Gittins JR, et al. Phytoplankton Calcification in a High-CO_2 World. Science. 2008; 320:336–40. https://doi.org/10.1126/science.1154122 PMID: 18420926
9. Alcolombri U, Ben-Dor S, Feldmesser E, Levin Y, Tawfik DS, Vardi A. Identification of the algal dimethyl sulfide–releasing enzyme: A missing link in the marine sulfur cycle. Science. 2015; 348(6242):1466–9. https://doi.org/10.1126/science.aab1586
10. Simo R. Production of atmospheric sulfur by oceanic plankton: biogeochemical, ecological and evolutionary links. Trends Ecol Evol. 2001; 16(6):287–94. PMID: 11369106
11. Bratbak G, Egge J, Heldal M. Viral mortality of the marine alga *Emiliania huxelyi* (Haptophyceae) and the termination of the algal bloom. Mar Ecol Prog Ser. 1993; 93:39–48.
12. Schroeder DC, Oke J, Malin G, Wilson WH. Coccolithovirus (*Phycodnaviridae*): characterisation of a new large dsDNA algal virus that infects *Emiliania huxleyi*. Arch Virol. 2002; 147:1685–98. https://doi.org/10.1007/s00705-002-0841-3 PMID: 12209309
13. Read BA, Kegel J, Klute MJ, Kuo A, Lefebvre SC, Maumus F, et al. Pan genome of the phytoplankton *Emiliania* underpins its global distribution. Nature. 2013; 499:209–13. https://doi.org/10.1038/nature12221 PMID: 23760476
14. Vardi A, Haramaty L, Van Mooy BA, Fredricks HF, Kimmance SA, Larsen A, et al. Host-virus dynamics and subcellular controls of cell fate in a natural coccolithophore population. Proc Natl Acad Sci USA. 2012; 109(47):19327–32. https://doi.org/10.1073/pnas.1208895109 PMID: 23134731
15. Bidle KD, Vardi A. A chemical arms race at sea mediates algal host–virus interactions. Curr Opin Microbiol. 2011; 14(4):449–57. http://dx.doi.org/10.1016/j.mib.2011.07.013. PMID: 21816665
16. Wilson WH, Schroeder DC, Allen MJ, Holden MTG, Parkhill J, Barrell BG, et al. Complete genome sequence and lytic phase transcription profile of a *Coccolithovirus*. Science. 2005; 309(5737):1090–2. https://doi.org/10.1126/science.1113109 PMID: 16099989
17. Feldmesser E, Rosenwasser S, Vardi A, Ben-Dor S. Improving transcriptome construction in non-model organisms: integrating manual and automated gene definition in *Emiliania huxleyi*. BMC Genomics. 2014; 15:148–63. https://doi.org/10.1186/1471-2164-15-148 PMID: 24559402
18. Rosenwasser S, Mausz MA, Schatz D, Sheyn U, Malitsky S, Aharoni A, et al. Rewiring host lipid metabolism by large viruses determines the fate of *Emiliania huxleyi*, a bloom-forming alga in the ocean. Plant Cell 2014; 26:2689–707. https://doi.org/10.1105/tpc.114.125641 PMID: 24920329
19. Zhang X, Gamarra J, Castro S, Carrasco E, Hernandez A, Mock T, et al. Characterization of the small RNA transcriptome of the marine coccolithophorid, *Emiliania Huxleyi*. PLoS One. 2016; 11(4): e0154279. https://doi.org/10.1371/journal.pone.0154279 PMID: 27101007
20. Schatz D, Rosenwasser S, Malitsky S, Wolf SG, Feldmesser E, Vardi A. Communication via extracellular vesicles enhances viral infection of a cosmopolitan alga. Nature Microbiology. 2017; 2(11):1485–92. https://doi.org/10.1038/s41564-017-0024-3 PMID: 28924189
21. Rosenwasser S, Ziv C, Creveld SGv, Vardi A. Virocell Metabolism: Metabolic innovations during host-virus interactions in the ocean. Trends Microbiol. 2016; 24:821–32. https://doi.org/10.1016/j.tim.2016.06.006 PMID: 27395772
22. Ankrah NYD, May AL, Middleton JL, Jones DR, Hadden MK, Gooding JR, et al. Phage infection of an environmentally relevant marine bacterium alters host metabolism and lysate composition. ISME J. 2014; 8(5):1089–100. https://doi.org/10.1038/ismej.2013.216 PMID: 24304672
23. Enav H, Mandel-Gutfreund Y, Beja O. Comparative metagenomic analyses reveal viral-induced shifts of host metabolism towards nucleotide biosynthesis. Microbiome. 2014; 2(1):9. https://doi.org/10.1186/2049-2618-2-9 PMID: 24666644
24. Hurwitz BL, Hallam SJ, Sullivan MB. Metabolic reprogramming by viruses in the sunlit and dark ocean. Genome Biol. 2013; 14(11):R123. https://doi.org/10.1186/gb-2013-14-11-r123 PMID: 24200126
25. De Smet J, Zimmermann M, Kogadeeva M, Ceyssens P-J, Vermaelen W, Blasdel B, et al. High coverage metabolomics analysis reveals phage-specific alterations to Pseudomonas aeruginosa physiology during infection. ISME J. 2016. https://doi.org/10.1038/ismej.2016.3 PMID: 26882266
26. Thompson LR, Zeng Q, Kelly L, Huang KH, Singer AU, Stubbe J, et al. Phage auxiliary metabolic genes and the redirection of cyanobacterial host carbon metabolism. Proc Natl Acad Sci USA. 2011; 108(39): E757–64. https://doi.org/10.1073/pnas.1102164108 PMID: 21844365
27. Malitsky S, Ziv C, Rosenwasser S, Zheng S, Schatz D, Porat Z, et al. Viral infection of the marine alga *Emiliania huxleyi* triggers lipidome remodeling and induces the production of highly saturated triacylglycerol. New Phytol. 2016; 210(1):88–96. https://doi.org/10.1111/nph.13852 PMID: 26856244
28. Lehahn Y, Koren I, Schatz D, Frada M, Sheyn U, Boss E, et al. Decoupling physical from biological processes to assess the impact of viruses on a mesoscale algal bloom. Curr Biol. 2014; 24(17):2041–6. http://dx.doi.org/10.1016/j.cub.2014.07.046. PMID: 25155511

29. Mackinder LC, Worthy CA, Biggi G, Hall M, Ryan KP, Varsani A, et al. A unicellular algal virus, *Emiliania huxleyi* virus 86, exploits an animal-like infection strategy. J. Gen. Virol. 2009; 90(9):2306–16. https://doi.org/10.1099/vir.0.011635-0

30. Ziv C, Malitsky S, Othman A, Ben-Dor S, Wei Y, Zheng S, et al. Viral serine palmitoyltransferase induces metabolic switch in sphingolipid biosynthesis and is required for infection of a marine alga. Proc Natl Acad Sci USA. 2016; 113: E1907–E16. https://doi.org/10.1073/pnas.1523168113 PMID: 26984500

31. Vardi A, Van Mooy BA, Fredricks HF, Popendorf KJ, Ossolinski JE, Haramaty L, et al. Viral glycosphingolipids induce lytic infection and cell death in marine phytoplankton. Science. 2009; 326(5954):861–5. https://doi.org/10.1126/science.1177322 PMID: 19892986

32. Bidle KD, Haramaty L, Barcelos e Ramos J, Falkowski P. Viral activation and recruitment of metacaspases in the unicellular coccolithophore, *Emiliania huxleyi*. Proc Natl Acad Sci USA. 2007; 104 (14):6049–54. https://doi.org/10.1073/pnas.0701240104 PMID: 17392426

33. Sheyn U, Rosenwasser S, Ben-Dor S, Porat Z, Vardi A. Modulation of host ROS metabolism is essential for viral infection of a bloom forming coccolithophore in the ocean. ISME J. 2016; 10:1742–54. https://doi.org/10.1038/ismej.2015.228 PMID: 26784355

34. Schatz D, Shemi A, Rosenwasser S, Sabanay H, Wolf SG, Ben-Dor S, et al. Hijacking of an autophagy-like process is critical for the life cycle of a DNA virus infecting oceanic algal blooms. New Phytol. 2014; 204(4):854–63. https://doi.org/10.1111/nph.13008 PMID: 25195618

35. Cheng Y-S, Labavitch J, VanderGheynst JS. Organic and inorganic nitrogen impact chlorella variabilis productivity and host quality for viral production and cell lysis. Appl Biochem Biotechnol. 2015; 176 (2):467–79. https://doi.org/10.1007/s12010-015-1588-0 PMID: 25805020

36. Colson P, De Lamballerie X, Yutin N, Asgari S, Bigot Y, Bideshi DK, et al. "Megavirales", a proposed new order for eukaryotic nucleocytoplasmic large DNA viruses. Arch Virol. 2013; 158(12):2517–21. https://doi.org/10.1007/s00705-013-1768-6 PMID: 23812617

37. Forterre P. To be or not to be alive: How recent discoveries challenge the traditional definitions of viruses and life. Stud Hist Philos Biol Biomed Sci. 2016; 59:100–8. http://dx.doi.org/10.1016/j.shpsc.2016.02.013. PMID: 26996409

38. Frada M, Probert I, Allen MJ, Wilson WH, de Vargas C. The "Cheshire Cat" escape strategy of the coccolithophore *Emiliania huxleyi* in response to viral infection. Proc Natl Acad Sci USA. 2008; 105 (41):15944–9. https://doi.org/10.1073/pnas.0807707105 PMID: 18824682

39. Kashtan N, Roggensack SE, Rodrigue S, Thompson JW, Biller SJ, Coe A, et al. Single-cell genomics reveals hundreds of coexisting subpopulations in wild prochlorococcus. Science. 2014; 344(6182):416–20. https://doi.org/10.1126/science.1248575 PMID: 24763590

40. Yoon HS, Price DC, Stepanauskas R, Rajah VD, Sieracki ME, Wilson WH, et al. Single-cell genomics reveals organismal interactions in uncultivated marine protists. Science. 2011; 332(6030):714–7. https://doi.org/10.1126/science.1203163 PMID: 21551060

41. Ackermann M. A functional perspective on phenotypic heterogeneity in microorganisms. Nature Reviews Microbiology. 2015; 13:497. https://doi.org/10.1038/nrmicro3491 PMID: 26145732

42. Liu S, Trapnell C. Single-cell transcriptome sequencing: recent advances and remaining challenges. F1000Research 2016; 5.

43. Guillaume-Gentil O, Grindberg RV, Kooger R, Dorwling-Carter L, Martinez V, Ossola D, et al. Tunable single-cell extraction for molecular analyses. Cell. 166(2):506–16. https://doi.org/10.1016/j.cell.2016.06.025 PMID: 27419874

44. Tang F, Barbacioru C, Wang Y, Nordman E, Lee C, Xu N, et al. mRNA-Seq whole-transcriptome analysis of a single cell. Nat Meth. 2009; 6(5):377–82.

45. Hashimshony T, Wagner F, Sher N, Yanai I. CEL-Seq: Single-cell rna-seq by multiplexed linear amplification. Cell Reports. 2012; 2(3):666–73. http://dx.doi.org/10.1016/j.celrep.2012.08.003. PMID: 22939981

46. Grun D, Lyubimova A, Kester L, Wiebrands K, Basak O, Sasaki N, et al. Single-cell messenger RNA sequencing reveals rare intestinal cell types. Nature. 2015; 525(7568):251–5. https://doi.org/10.1038/nature14966 PMID: 26287467

47. Zeisel A, Muñoz-Manchado AB, Codeluppi S, Lönnerberg P, La Manno G, Juréus A, et al. Cell types in the mouse cortex and hippocampus revealed by single-cell RNA-seq. Science. 2015; 347(6226):1138–42. https://doi.org/10.1126/science.aaa1934 PMID: 25700174

48. Efroni I, Mello A, Nawy T, Ip P-L, Rahni R, DelRose N, et al. Root Regeneration Triggers an Embryo-like Sequence Guided by Hormonal Interactions. Cell. 2016; 165(7):1721–33. https://doi.org/10.1016/j.cell.2016.04.046 PMID: 27212234

49. Avraham R, Haseley N, Brown D, Penaranda C, Jijon HB, Trombetta JJ, et al. Pathogen cell-to-cell variability drives heterogeneity in host immune responses. Cell. 163(2):523. https://doi.org/10.1016/j.cell.2015.09.044

50. Shalek AK, Satija R, Shuga J, Trombetta JJ, Gennert D, Lu D, et al. Single-cell RNA-seq reveals dynamic paracrine control of cellular variation. Nature. 2014; 510(7505):363–9. https://doi.org/10.1038/nature13437 PMID: 24919153

51. Saliba A-E, Li L, Westermann AJ, Appenzeller S, Stapels DAC, Schulte LN, et al. Single-cell RNA-seq ties macrophage polarization to growth rate of intracellular Salmonella. Nature Microbiol. 2016; 2:16206. https://doi.org/10.1038/nmicrobiol.2016.206 PMID: 27841856

52. Patil S, Fribourg M, Ge Y, Batish M, Tyagi S, Hayot F, et al. Single-cell analysis shows that paracrine signaling by first responder cells shapes the interferon-β response to viral infection. Sci Signal. 2015; 8(363):ra16–ra. https://doi.org/10.1126/scisignal.2005728 PMID: 25670204

53. Snijder B, Sacher R, Ramo P, Damm E-M, Liberali P, Pelkmans L. Population context determines cell-to-cell variability in endocytosis and virus infection. Nature. 2009; 461(7263):520–3. https://doi.org/10.1038/nature08282 PMID: 19710653

54. Heldt FS, Kupke SY, Dorl S, Reichl U, Frensing T. Single-cell analysis and stochastic modelling unveil large cell-to-cell variability in influenza A virus infection. Nat Comm. 2015; 6:8938. https://doi.org/10.1038/ncomms9938 PMID: 26586423

55. Cohen EM, Kobiler O. Gene expression correlates with the number of herpes viral genomes initiating infection in single cells. PLOS Pathog. 2016; 12(12):e1006082. https://doi.org/10.1371/journal.ppat.1006082 PMID: 27923068

56. Russell AB, Trapnell C, Bloom JD. Extreme heterogeneity of influenza virus infection in single cells. eLife. 2018; 7:e32303. https://doi.org/10.7554/eLife.32303 PMID: 29451492

57. Zanini F, Pu S-Y, Bekerman E, Einav S, Quake SR. Single-cell transcriptional dynamics of flavivirus infection. eLife. 2018; 7:e32942. https://doi.org/10.7554/eLife.32942 PMID: 29451494

58. Guo F, Li S, Caglar MU, Mao Z, Liu W, Woodman A, et al. Single-Cell Virology: On-chip investigation of viral infection dynamics. Cell Reports. 2017; 21(6):1692–704. https://doi.org/10.1016/j.celrep.2017.10.051 PMID: 29117571

59. Westermann AJ, Gorski SA, Vogel J. Dual RNA-seq of pathogen and host. Nat Rev Micro. 2012; 10(9):618–30.

60. Rosani U, Varotto L, Domeneghetti S, Arcangeli G, Pallavicini A, Venier P. Dual analysis of host and pathogen transcriptomes in ostreid herpesvirus 1-positive Crassostrea gigas. Environ Microbiol 2015; 17(11):4200–12. https://doi.org/10.1111/1462-2920.12706 PMID: 25384719

61. Nuss AM, Beckstette M, Pimenova M, Schmühl C, Opitz W, Pisano F, et al. Tissue dual RNA-seq allows fast discovery of infection-specific functions and riboregulators shaping host–pathogen transcriptomes. Proc Natl Acad Sci USA. 2017; 114(5):E791–E800. https://doi.org/10.1073/pnas.1613405114 PMID: 28096329

62. Allen MJ, Forster T, Schroeder DC, Hall M, Roy D, Ghazal P, et al. Locus-specific gene expression pattern suggests a unique propagation strategy for a giant algal virus. J Virol. 2006; 80(15):7699–705. https://doi.org/10.1128/JVI.00491-06 PMID: 16840348

63. Frada MJ, Rosenwasser S, Ben-Dor S, Shemi A, Sabanay H, Vardi A. Morphological switch to a resistant subpopulation in response to viral infection in the bloom-forming coccolithophore Emiliania huxleyi. PLOS Patho. 2017; 13(12):e1006775. https://doi.org/10.1371/journal.ppat.1006775 PMID: 29244854

64. Wu AR, Neff NF, Kalisky T, Dalerba P, Treutlein B, Rothenberg ME, et al. Quantitative assessment of single-cell RNA-sequencing methods. Nat Meth. 2014; 11(1):41–6. https://doi.org/10.1038/nmeth.2694 PMID: 24141493

65. McDavid A, Finak G, Chattopadyay PK, Dominguez M, Lamoreaux L, Ma SS, et al. Data exploration, quality control and testing in single-cell qPCR-based gene expression experiments. Bioinformatics. 2013; 29(4):461–7. https://doi.org/10.1093/bioinformatics/bts714 PMID: 23267174

66. Thingstad TF. Elements of a theory for the mechanisms controlling abundance, diversity, and biogeochemical role of lytic bacterial viruses in aquatic systems. Limnol Oceanog. 2000; 45(6):1320–8. https://doi.org/10.4319/lo.2000.45.6.1320

67. Thyrhaug R, Larsen A, Thingstad FT, Bratbak G. Stable coexistence in marine algal host-virus systems. Mar Ecol Prog Ser. 2003; 254:27–35.

68. Schreiber F, Littmann S, Lavik G, Escrig S, Meibom A, Kuypers MMM, et al. Phenotypic heterogeneity driven by nutrient limitation promotes growth in fluctuating environments. Nat Microbiol. 2016; 1:16055. https://doi.org/10.1038/nmicrobiol.2016.55 PMID: 27572840

69. Martínez JM, Schroeder DC, Larsen A, Bratbak G, Wilson WH. Molecular dynamics of emiliania huxleyi and cooccurring viruses during two separate mesocosm studies. Appl Environ Microbiol. 2007; 73(2):554–62. https://doi.org/10.1128/AEM.00864-06 PMID: 17098923

70. Maat DS, Crawfurd KJ, Timmermans KR, Brussaard CPD. Elevated co_2 and phosphate limitation favor micromonas pusilla through stimulated growth and reduced viral impact. Appl Environ Microbiol. 2014; 80(10):3119–27. https://doi.org/10.1128/AEM.03639-13 PMID: 24610859

71. Thamatrakoln K, Talmy D, Haramaty L, Maniscalco C, Latham JR, Knowles B, et al. Light regulation of coccolithophore host–virus interactions. New Phytologist. 2018. https://doi.org/10.1111/nph.15459 PMID: 30368816

72. Barak-Gavish N, Frada MJ, Lee PA, DiTullio GR, Ku C, Malitsky S, et al. Bacterial virulence against an oceanic bloom-forming phytoplankter is mediated by algal DMSP. Sci Adv. 2018. https://doi.org/10.1126/sciadv.aau5716 PMID: 30397652

73. Mausz MA, Pohnert G. Phenotypic diversity of diploid and haploid *Emiliania huxleyi* cells and of cells in different growth phases revealed by comparative metabolomics. J Plant Physiol. 2015; 172:137–48. https://doi.org/10.1016/j.jplph.2014.05.014 PMID: 25304662

74. Hunter JE, Frada MJ, Fredricks HF, Vardi A, Van Mooy BAS. Targeted and untargeted lipidomics of *Emiliania huxleyi* viral infection and life cycle phases highlights molecular biomarkers of infection, susceptibility, and ploidy. Front Mar Sci. 2015; 2(81). https://doi.org/10.3389/fmars.2015.00081

75. Yau S, Hemon C, Derelle E, Moreau H, Piganeau G, Grimsley N. A Viral immunity chromosome in the marine picoeukaryote, *Ostreococcus tauri*. PLOS Pathog. 2016; 12(10):e1005965. https://doi.org/10.1371/journal.ppat.1005965 PMID: 27788272

76. Westermann AJ, Barquist L, Vogel J. Resolving host–pathogen interactions by dual RNA-seq. PLOS Pathog. 2017; 13(2):e1006033. https://doi.org/10.1371/journal.ppat.1006033 PMID: 28207848

77. Keller MD, Selvin RC, Claus W, Guillard RRL. Media for the culture of oceanic ultraphytoplankton. J Phycol. 1987; 23(4):633–8. https://doi.org/10.1111/j.1529-8817.1987.tb04217.x